

Chan SC, Kendon EJ, Roberts NM, Fowler HJ, Blenkinsop S.  
[Downturn in scaling of UK extreme rainfall with temperature for future hottest days.](#)

*Nature Geosciences* 2016, 9(1), 24-28.

**Copyright:**

This is the authors' accepted manuscript of an article that was published in its final definitive form by Nature Publishing Group, 2016.

**DOI link to article:**

<http://dx.doi.org/10.1038/NGEO2596>

**Date deposited:**

19/08/2016

1 Downturn in scaling of UK extreme rainfall  
2 with temperature for future hottest days

3 Steven C. Chan<sup>1</sup>, Elizabeth J. Kendon<sup>2</sup>, Nigel M. Roberts<sup>3</sup>,  
4 Hayley J. Fowler<sup>1</sup>, & Stephen Blenkinsop<sup>1</sup>

5 October 15, 2015

6 <sup>1</sup>*School of Civil Engineering & Geosciences, Newcastle University, Newcastle-*  
7 *upon-Tyne, United Kingdom*

8 <sup>2</sup>*Met Office Hadley Centre, Exeter, United Kingdom*

9 <sup>3</sup>*MetOffice@Reading, Reading, United Kingdom*

10 **Extreme daily precipitation is thought to increase with tempera-**  
11 **ture at a rate of 6.5% per K according to the Clausius-Clapeyron**  
12 **relationship between temperature and saturation vapour pressure**  
13 **[1]. A wide range of scaling relationships has been observed glob-**  
14 **ally for extreme daily and hourly precipitation, with evidence of**  
15 **scaling above 6.5% per K for sub-daily extreme precipitation in**  
16 **some regions [2, 3, 4]. Only high-resolution climate models can**  
17 **simulate this scaling relationship [5]. Here we examine the scaling**  
18 **of hourly extreme precipitation intensities in a future climate, us-**  
19 **ing experiments with a model for the southern UK with kilometre-**  
20 **scale resolution [6]. Our model simulates the present-day scaling**  
21 **relationship at 6.5% per K, in agreement with observations. The**  
22 **simulated overall future increase in extreme precipitation follows**  
23 **the same relationship. However, UK extreme precipitation inten-**  
24 **sities decline at temperatures above about 22°C – a temperature**  
25 **range that is not well sampled in the present-day integration –**  
26 **as a result of a more frequent occurrence of anticyclonic weather**  
27 **systems. Anticyclones produce more days with strong daytime**

28 heating, but are not favourable to the development of deep intense  
29 convective storms. We conclude that future extreme hourly precip-  
30 itation intensities cannot simply be extrapolated from present-day  
31 temperature scaling, and demonstrate the pitfalls of using regional  
32 surface temperature as a scaling variable.

33 The Clausius-Clapeyron (C-C; see Supplementary Information) relation  
34 describes the rate of change of saturated vapour pressure with temperature.  
35 For water vapour, this is  $\approx 6\text{--}7\%$  per K near the Earth surface. Assum-  
36 ing constant relative humidity (RH), this sets a scale for change in extreme  
37 daily precipitation intensities [1]. The observed relationship globally between  
38 annual maximum daily precipitation and global mean temperature is about  
39  $5.9\text{--}7.7\%$  per K, consistent with the C-C relation [7]. As a consequence,  
40 temperature changes become a potential predictor for extreme daily precip-  
41 itation change. Here we assume a C-C scaling of  $\gamma \approx 6.5\%$  per K. Changes  
42 in weather patterns, moisture availability [8] and thermodynamic stability  
43 [9, 10, 11] may lead to scalings that depart substantially from  $\gamma$ .

44 Most climate models require convective parameterisations (CP) to repre-  
45 sent convection, but CP is not designed to represent individual storms and  
46 their precipitation [12]. Even moderately high-resolution model versions are  
47 unable to replicate observed scaling at temperatures above  $20^\circ\text{C}$  [2]. Since  
48 warmer temperatures are typically associated with a greater proportion of  
49 convective compared to stratiform precipitation [13], the inadequacies of the  
50 model CP become increasingly important as temperature rises; such models  
51 are known to show inconsistent temperature and humidity changes [10, 14].  
52 However, a “convective-permitting” (no-CP) high-resolution regional climate  
53 model (RCM) is able to replicate observed super-C-C scaling for hourly pre-  
54 cipitation over the Alps for a present-day simulation [5].

55 The C-C hypothesis has been tested in many observational and mod-  
56 elling studies. General circulation model (GCM) projections produce sub-  
57 C-C scaling for daily mean precipitation; only daily extreme precipitation  
58 scalings are consistent with the C-C hypothesis [10, 11, 15, 16]. At regional  
59 and local scales, observed scalings of extreme hourly precipitation can ex-  
60 ceed  $\gamma$  (“super-scaling”) [2, 3]. Some studies have found super-scaling only  
61 for sub-hourly totals [4]. A decline in extreme hourly precipitation inten-  
62 sities at temperature exceeding  $\approx 23^\circ\text{C}$  is found in some subtropical and  
63 tropical regions [4, 17]. These previous studies have examined surface tem-  
64 perature and humidity as scaling variables because they are well observed.

65 However, surface conditions may be strongly modulated by solar heating,  
66 and do not necessarily provide useful information about the thermodynamic  
67 and dynamic properties of the storms. Studies looking at tropospheric ver-  
68 tical velocity and humidity have shown a positive scaling with extreme daily  
69 precipitation [10, 11]. For Europe, projections of summer daily and hourly  
70 extreme precipitation projections show both increases and decreases for dif-  
71 ferent parts of Europe [18, 19].

72 UK C-C scaling of extreme precipitation intensities has been examined  
73 in observations showing super-scaling for anti-cyclonic conditions in sum-  
74 mer [20], but the same has not been examined for model simulations. The  
75 UK Met Office (UKMO) has recently completed continuous high-resolution  
76 (convective-permitting 1.5-km southern UK and CP-enabled 12-km Euro-  
77 pean) present-day (G-P) and future-climate (G-F) RCM simulations [6, 21]  
78 with large-scale conditions provided by HadGEM3 GCM integrations [22].  
79 Despite larger mean precipitation biases, the 1.5-km model has significantly  
80 improved physical realism in simulating extreme precipitation intensities  
81 compared to coarser-resolution model simulations [21], and shows future in-  
82 tensification of both summer and winter extremes [6]. Here, we examine its  
83 ability to represent observed C-C scaling relationships for the southern UK  
84 from radar observations [23], and the extent to which these scalings may  
85 apply with future climate change.

86 Relationships between hourly extreme precipitation intensities and daily  
87 temperatures for summer (Jun-Jul-Aug; JJA) and winter (Dec-Jan-Feb; DJF)  
88 over southern UK land points are shown in Figure 1 for radar, present-day,  
89 and future-climate integrations. For summer, the 99<sup>th</sup> percentile precipi-  
90 tation increases in the radar observations at  $\gamma$  — the same rate as for UK  
91 gauge observations [20], and this scaling is only captured by the 1.5-km model  
92 (Figure 1b). The 12-km model is unable to capture the observed scaling, pro-  
93 ducing relatively constant intensities with temperature increases. However,  
94 both the 12-km and 1.5-km models are able to capture the observed scaling in  
95 winter (Figure 1d and e), which is less than  $\gamma$ . Neither observed nor present-  
96 day climate integrations show a clear relationship between temperature and  
97 extreme daily precipitation (see Supplementary Figure 1).

98 Unlike other analyses of observed data [2] and model simulations [5], there  
99 is little evidence of “super-scaling” in either radar observations or model sim-  
100 ulations for southern UK as an average, but local scaling variations do exist  
101 (see Supplementary Figure 2). We do not account for scaling variations un-  
102 der different weather regimes and conditions [13, 20]. However, the fact that

103 the 1.5-km model can capture the observed scaling gives us more confidence  
104 in its use to estimate future scalings.

105 Scaling relationships for future simulations are shown in the right panels  
106 of Figure 1. A  $\approx 5^\circ\text{C}$  warming and an average 30% increase for the 99<sup>th</sup>  
107 percentile of summer precipitation intensities for the 1.5-km model across  
108 the full temperature range is consistent with the C-C hypothesis. The Alps-  
109 region analysis [24] — examining the change in 99.9th percentile precipitation  
110 extreme between control and future simulations — provides a smaller 3 –  
111 6% change. However, unlike our “wet”-value-only analysis, they use both  
112 “wet” and “dry” values to calculate percentiles; therefore, the changes reflect  
113 a combination of changes in both frequency and intensity. For the future  
114 climate, we find both the 1.5-km and 12-km models simulate declines in  
115 hourly extreme precipitation intensities at temperatures in excess of  $\approx 22^\circ\text{C}$   
116 over the southern UK. Such declines have been observed globally for daily  
117 intensities, whereas hourly precipitation declines are mostly found in the  
118 subtropics and tropics [4, 17]. The UK declines occur at the higher end  
119 of the future temperature range, which is not sampled in the present-day  
120 climate simulations. Over the overlapping temperature range, the scaling  
121 of the 1.5-km future-climate simulation is comparable with the present-day  
122 simulation.

123 A warmer future climate may indeed be more favourable to extreme pre-  
124 cipitation, but our simulations indicate that this does not extend to the  
125 warmest summer days as seen in observational and modelling studies [4, 14].  
126 Two explanations have been put forward for the declines in the observed scal-  
127 ing relation at high temperatures: i) the decrease in extreme precipitation  
128 event duration [4]; ii) the suppression of RH [17]. For the former, sub-hourly  
129 extreme precipitation intensities continue to intensify with temperature in-  
130 creases [4]. For the latter, a decrease in RH has been found over land since  
131 the late 1990s [25], and climate models project reductions in extra-tropical  
132 troposphere RH [26]. Here, we examine the role of RH.

133 Precipitation totals are ultimately constrained by moisture availability,  
134 which may be much less than the temperature-dependent maximum. Here  
135 we turn to the near-surface dew point  $T_d$  [14], and wet-bulb potential tem-  
136 perature  $\theta_w$  as humidity measures (see Methods). In Figure 2, we plot the  
137 variation of the 99<sup>th</sup> percentile of 1-hour summer precipitation ( $P_{1\text{-hr}}$ ) with  
138 near-surface  $T_d$  and 850-hPa  $\theta_w$  for both the 1.5-km and 12-km models. Un-  
139 like Figure 1, the results here are obtained using a “non-local” method —  
140 whereby the highest near-surface  $T_d$  and 850-hPa  $\theta_w$  is found near the pre-

141 cipitating grid point (see Methods).

142 Both models sample a similar range of  $T_d$  and 850-hPa  $\theta_w$ . All but the  
143 future 12-km simulation show increases of extreme hourly precipitation in-  
144 tensities with  $T_d$  and  $\theta_w$  in accordance with the  $\gamma$  scaling. For near-surface  
145  $T_d$ , the scaling here is less than previous work [14]; a full discussion is in  
146 the Supplementary Information, including justification for the “non-local”  
147 methodology and the usage of 850-hPa  $\theta_w$ . The 1.5-km future simulation  
148 shows a general extension of the  $\gamma$  scaling for the present-day climate into  
149 a higher  $T_d$  and  $\theta_w$  range. This extension is similar for the 12-km model,  
150 however at the highest  $T_d$  ( $18 + ^\circ\text{C}$ ), extreme hourly precipitation intensities  
151 decline with  $T_d$ .

152 The scaling decline for the 12-km RCM is not seen with 850-hPa  $\theta_w$ , but is  
153 evident with 850-hPa temperatures and local surface dew points (Supplemen-  
154 tary Figure 3 and 4). The differences are likely related to the use of CP by  
155 the 12-km model [10], but a detailed examination is beyond the scope of this  
156 paper. Nevertheless, results indicate model-simulated scalings with upper-air  
157 humidities and temperatures are generally more consistent than the scalings  
158 with surface humidities and temperatures. For the 1.5-km RCM, the hot  
159 day scaling declines in the future simulations are associated with reduced-  
160 RH days and thus a higher saturation barrier. Model-simulated relationships  
161 between precipitation,  $\theta_w$  and surface air temperature are explored further  
162 in Supplementary Figure 5.

163 Since the large-scale flow influences local weather conditions, we use mean  
164 sea-level pressure (MSLP) as a diagnostic for examining that influence. In  
165 Figure 3, we plot the differences in model-simulated MSLP between wet days  
166 with high surface air temperature and wet days with high  $\theta_w$ . Compared to  
167 wet-high  $\theta_w$  days, wet-hot days over the southern UK are associated with  
168 higher MSLP anomalies. The positive MSLP anomalies are indicative of  
169 less fronts [27], more anticyclonic conditions with drier and hotter weather,  
170 reducing RH, and inhibiting deep convection. The MSLP anomalies also  
171 suggest weaker low-level westerlies over much of the UK, and imply reduced  
172 moisture from the warm Atlantic (Supplementary Figure 6). Changes in  
173 MSLP between the future- and present-day integrations reveal a shift to more  
174 anticyclonic conditions over the UK in the future (Supplementary Figure 7).  
175 This change comes from the driving GCM, and appears to be the driver of  
176 the downturn in scaling at high temperatures in the 1.5-km RCM through  
177 its effect on reducing absolute and relative humidity. Such anticyclonic shifts  
178 are found in other GCM projections for Europe, suggesting this downturn

179 may be a general feature of projections for this region and potentially other  
180 regions with similar shifts (see Supplementary Information).

181 In conclusion, we have shown that the 1.5-km convective-permitting RCM  
182 can simulate UK observed C-C scaling of hourly extreme precipitation inten-  
183 sities. This is true in both summer and winter, unlike the lower-resolution  
184 12-km RCM, which is only able to simulate the winter scaling. Despite  
185 an average intensification of extreme precipitation at  $\gamma$ , present-day hourly-  
186 precipitation scaling does not extend into higher temperatures ( $22 + ^\circ\text{C}$ )  
187 sampled only by the future climate integration. In particular, for surface  
188 temperatures exceeding  $\approx 22^\circ\text{C}$ , hourly extreme precipitation declines with  
189 increasing temperature. This breakdown in scaling has been observed around  
190 the globe for sub-daily and daily extreme precipitation. It, therefore, has im-  
191 plications for precipitation intensities globally as well as the UK.

192 We have demonstrated that 850-hPa  $\theta_w$  is an improved predictor for  
193 changes in precipitation extremes as it can account for relative humidity  
194 changes, giving a more consistent scaling between future- and present-day  
195 climate integrations compared to surface temperatures and dew points. The  
196 C-C hypothesis assumes that moisture availability is temperature limited,  
197 but our simulations indicate that, at the regional scale, weather patterns  
198 provide important moderators of moisture availability.

199 In the case of the UK under global warming, the driving GCM simulates  
200 a shift to a more anticyclonic MSLP regime causing more very hot days and  
201 less convection. Similar changes may also be a factor for observed declines  
202 in scaling at lower latitudes [4, 17]. We conclude that although changes  
203 to extreme hourly precipitation are dominated by thermodynamic changes,  
204 dynamical changes can have important regional effects. Therefore, regional  
205 surface temperatures cannot be used alone to extrapolate changes in extreme  
206 precipitation intensity. Realistic large-scale circulation patterns and variabil-  
207 ity from GCMs will be crucial for good regional predictions.

208 **Correspondence** Correspondence and requests for materials should be address-  
209 ed to Steven C Chan (email: [steven.chan@metoffice.gov.uk](mailto:steven.chan@metoffice.gov.uk)).

210 **Acknowledgements** This research is part of the projects CONVEX and IN-  
211 TENSE, and UKMO Hadley Centre research programme, which are supported by  
212 the United Kingdom NERC Changing Water Cycle programme (grant: NE/I0066-  
213 80/1), European Research Council (grant: ERC-2013-CoG), and the Joint De-  
214 partment of Energy and Climate Change and Department for Environment Food

215 and Rural Affairs (grant: GA01101), respectively. The lead author is financially  
216 supported by Newcastle University, and is a visiting scientist at the Met Office  
217 Hadley Centre. Hayley J. Fowler is funded by the Wolfson Foundation and the  
218 Royal Society as a Royal Society Wolfson Research Merit Award (WM140025)  
219 holder. Significant portions of the analysis are carried out with the free-and-open-  
220 source statistical software R and its add-on library packages. We would also like  
221 to thank Christopher A Ferro of the University of Exeter, Malcolm J. Roberts and  
222 Jonathan Wilkinson of the Met Office, and Wilfran Moufouma-Okia of the United  
223 Nations Economic Commission for Africa (formerly Met Office) for their valuable  
224 inputs to this work.

225 **Author Contributions** SCC co-wrote the manuscript, conducted data anal-  
226 ysis and data visualisation. EJK co-wrote the manuscript, supplied the data,  
227 performed the necessary model simulations, and advised on data analysis method-  
228 ologies and result interpretation. NMR co-wrote the manuscript, and advised on  
229 analysis methodologies and result interpretation. HJF advised on the analysis  
230 methodologies, discussed the results, co-wrote the manuscript, and commented  
231 on the manuscript. SB advised on observational aspects of the present study,  
232 discussed the results, and commented on the manuscript.

233 **Competing Interests** None

## 234 **Methods**

235 The UKMO high-resolution 1.5- and 12-km RCM simulations used in the  
236 present analysis have been fully described in other papers [6, 21]. The 1.5-km  
237 model simulations are centred over the southern United Kingdom [21] with an  
238 inner domain that roughly follows Supplementary Figure 2. Unlike the 12-km  
239 RCM, the 1.5-km model does not use convective parameterisation (CP), and  
240 is able to explicitly represent individual showers or storms on the model grid.  
241 The 1.5-km simulations are driven by 12-km European-domain simulations  
242 (also analysed here), which themselves are driven by 60-km HadGEM3 GCM  
243 simulations for the present- and future-climate. The future HadGEM3 sim-  
244 ulation follows the IPCC Representative Concentration Pathway 8.5W/m<sup>2</sup>  
245 “business as usual” climate forcing scenario for the end of 21st century [28].  
246 There is no ocean model coupling; future sea surface temperatures (SST)  
247 are superposition of another coupled model’s SST projections and observed



248 SSTs between 1997 and 2009, in which the latter serves as the SST baseline  
 249 that drives the present-climate GCM simulation [22]. The analysis domain is  
 250 the same as in previous studies [21]. Only land points are examined. Results  
 251 here focus on hourly precipitation; model-simulated sub-hourly precipitation  
 252 was unavailable to test duration changes [4], and may be examined in future  
 253 work.

254 For observed near-surface air temperature, we have used the National Cli-  
 255 mate Information Centre 5-km gridded daily temperature observations [UK5;  
 256 29]. Daily maximum ( $T_{\max}$ ) and minimum ( $T_{\min}$ ) surface air temperatures  
 257 are available from 1960, but we only use the data that overlap with the radar  
 258 period. The daily-averaged surface air temperatures ( $T_{\text{avg}}$ ) are estimated by:

$$T_{\text{avg}} = \frac{T_{\max} + T_{\min}}{2} \quad (1)$$

259 The UK5 daily values are taken between 09Z - 09Z. The RCM-simulated  
 260 daily averaged near-surface air temperature is computed with the same for-  
 261 mulation. However, UKMO models use a 00Z - 24Z period to determine daily  
 262 minimums and maximums.

263 For gridded hourly precipitation, we have used the UKMO gridded qual-  
 264 ity - controlled gauge - calibrated Radarnet composite radar observations,  
 265 which are available from 2003 [23]. Hence, our observational temperature-  
 266 precipitation analysis only covers the 2003-2012 period. The same radar  
 267 data have been previously used to examine UK precipitation extremes, and  
 268 a discussion of the pros and cons for using radar for climate research can be  
 269 found there and in other related papers [30, 31]. On average, radar tends to  
 270 underestimate intensities of intense rainfall due to attenuation of the beam  
 271 [23]. As in previous studies [2, 14, 17], we use the daily maximum of 1-hour  
 272 total precipitation  $P_{\max,1\text{-hr}}$  with a “wet” threshold of 0.1mm/hr. A minimum  
 273 “wet” threshold is adopted as we wish to separate intensity and frequency  
 274 changes [19]. It is the intensity which has been hypothesised to scale with  
 275 saturation vapour pressure, whilst frequency is less clearly related [1]. To be  
 276 consistent with the air temperature data, the daily window for  $P_{\max,1\text{-hr}}$  is as  
 277 for  $T_{\max}$  and  $T_{\min}$ . All data are first interpolated to a common 12-km grid  
 278 prior to any analysis including the selection of  $P_{\max,1\text{-hr}}$ . Spatial averaging is  
 279 used to interpolate precipitation.

280 For the C-C scaling analysis, the methodology used for Figure 1 is based

281 on the equal-sample-size binning method that is used in an Australian obser-  
282 vational study [17], but modifications of the original methodology are applied  
283 for gridded data. Here  $P_{\max,1\text{-hr}}$  values at each grid point and its eight neigh-  
284 bouring grid points are binned according to their “local” (central grid point)  
285  $T_{\text{avg}}$ . Each bin has a distribution of  $P_{\max,1\text{-hr}}$  values from which its percentiles  
286 are estimated. The temperature dependency of the percentiles can be then  
287 estimated. We require each  $T_{\text{avg}}$  bin to have approximately an equal number  
288 of data pairs.

289 The key differences with the Australian work are:

- 290 • We have used shorter datasets that are gridded. We conduct 3-by-3  
291 adjacent-grid-point pooling to increase our sample size, and the binning  
292 is conducted with the pooled samples
- 293 • We use 20 bins instead of the 12 bins used in the Australian study

294 The overall scaling relationship for the southern UK is estimated by super-  
295 posing all individual 3-by-3 grid-box relationships using hexagon scatter den-  
296 sity plots, and fitting a LOcally-wEighted Scatterplot Smoothing (LOESS)  
297 non-parametric regression line [4, 32]. We stratify our data by seasons (sum-  
298 mer and winter) to gain some separation between summer convective pre-  
299 cipitation and winter large-scale precipitation [17, 33]. The above method  
300 diagnoses scaling changes with temperature variability within a stationary  
301 (present or future) climate regime, and differs with the Alps-region future-  
302 climate projection analysis [24] which focuses on average percentile changes  
303 between the future and present climate.

304 Surface dew point temperature  $T_d$  is a measure of surface specific hu-  
305 midity translated to temperature with the C-C relationship [14]. Wet-bulb  
306 potential temperature  $\theta_w$  is a combined temperature-humidity measure that  
307 is unaffected by adiabatic motion or phase changes, and is commonly used  
308 in weather forecasting as an air mass indicator (see Supplementary Informa-  
309 tion). Model-simulated  $\theta_w$  and surface  $T_d$  are available every 6 hours and day  
310 respectively. To estimate the scaling relationship with  $\theta_w$  and surface dew  
311 point ( $T_d$ ) in Figure 2, we adopt the following approach. For each 6-hourly  
312 period, we first select the maximum over-land 1-hr precipitation within our  
313 region of interest ( $P_{1\text{-hr}}$ ; same 0.1mm/hr “wet” threshold applies). We then

314 determine the largest 850-hPa  $\theta_w$  or  $T_d$  in a 7-by-7 box centred over the se-  
315 lected grid point. The surface air temperature under the precipitating grid  
316 box is recorded for Figure 3. The key difference with the method we have  
317 used for temperature is that there is only one precipitation-( $\theta_w$ -or- $T_d$ ) pair  
318 per 6-hour period as opposed to as many pairs as precipitating grid boxes per  
319 day. The goal is to associate a precipitation intensity with a  $\theta_w$  or  $T_d$  that  
320 is representative of the air mass supplying the cloud. After all precipitation-  
321 ( $\theta_w$ -or- $T_d$ ) pairs are collected, the pairs are binned according to their  $\theta_w$  or  
322  $T_d$ . Bins with fewer than 200 samples are eliminated. The 95% confidence  
323 intervals (CI) of the percentile are estimated by “bootstrapping” [34]:

- 324 1. Randomly draw bin samples with replacement to create a new bin with  
325 the same number of samples; this is completed 5000 times
- 326 2. 5000 new percentiles are estimated
- 327 3. The 95% CI is taken to be the 2.5% and 97.5% percentiles from the  
328 new 5000 estimates

329 The above method departs from the temperature-precipitation analysis  
330 to reduce double counting: each precipitating grid point — possibly from  
331 the same precipitating system — would find a common non-local  $\theta_w$  maxi-  
332 mum. Double counting would cause erroneous uncertainty underestimation  
333 and over-confidence of the presented results. However, the sample number  
334 for one value per 6 hours is substantially less than using all wet values per  
335 wet day if one assumes there are at least 4 wet land grid points per wet day.  
336 Sensitivity tests have shown that results do not change substantially at lower  
337 isobaric level (925-hPa), and  $\theta_w$  box sizes are chosen by gradual increase of  
338 box size until results are stabilised. The non-local method is adopted as the  
339 existence of precipitation and clouds are likely to modify “local”  $\theta_w$  and  $T_d$ .  
340 The non-local method aims to sample more representative values for  $\theta_w$  and  
341  $T_d$  that are being fed into the cloud.

342 Code availability. The R and IDL source code used in the analysis can  
343 be requested from the lead author, but installations of additional software  
344 packages may be required. R is available as free-and-open-source software,  
345 and IDL is a propriety product available from Exelis Visual Information  
346 Solutions [35, 36]. The model and observational data used are under Crown

347 copyright of the UK Met Office, and access may be requested from the Met  
348 Office.

## 349 **References**

- 350 [1] Trenberth, K. E., Dai, A., Rasmussen, R. M. & Parsons, D. B. The  
351 changing character of precipitation. *Bull. Am. Meteorol. Soc.* **84**, 1205–  
352 1217 (2003).
- 353 [2] Lenderink, G. & van Meijgaard, E. Increase in hourly precipitation ex-  
354 tremes beyond expectations from temperature changes. *Nature Geosci.*  
355 **1**, 511–514 (2008).
- 356 [3] Berg, P., Moseley, C. & Haerter, J. O. Strong increase in convective  
357 precipitation in response to higher temperatures. *Nature Geosci.* **6**,  
358 181–185 (2013).
- 359 [4] Utsumi, N., Seto, S., Kanae, S., Maeda, E. E. & Oki, T. Does higher  
360 surface temperature intensify extreme precipitation? *Geophys. Res.*  
361 *Lett.* **38**, L16708 (2011).
- 362 [5] Ban, N., Schmidli, J. & Schär, C. Evaluation of the convection-resolving  
363 regional climate modeling approach in decade-long simulations. *J. Geo-*  
364 *phys. Res.* **119**, 7889–7907 (2014).
- 365 [6] Kendon, E. J. *et al.* Heavier summer downpours with climate change  
366 revealed by weather forecast resolution model. *Nature Climate Change*  
367 **4**, 570–576 (2014).
- 368 [7] Westra, S., Alexander, L. V. & Zwiers, F. W. Global increasing trends in  
369 annual maximum daily precipitation. *J. Climate* **26**, 3904–3918 (2013).
- 370 [8] Dai, A. Recent climatology, variability, and trends in global surface  
371 humidity. *J. Climate* **19**, 3589–3606 (2006).
- 372 [9] Schneider, T. & O’Gorman, P. A. Moist convection and the thermal  
373 stratification of the extratropical troposphere. *J. Atmos. Sci.* **65**, 3571–  
374 3583 (2008).

- 375 [10] OGorman, P. A. & Schneider, T. The physical basis for increases in  
376 precipitation extremes in simulations of 21st-century climate change.  
377 *Proc. Natl. Acad. Sci. USA* **106**, 14773–14777 (2009).
- 378 [11] Sugiyama, M., Shiogama, H. & Emori, S. Precipitation extreme changes  
379 exceeding moisture content increases in miroc and ipcc climate models.  
380 *Proc. Natl. Acad. Sci. USA* **107**, 571–575 (2009).
- 381 [12] Arakawa, A. The cumulus parameterization problem: Past, present, and  
382 future. *J. Climate* **17**, 2493–2525 (2004).
- 383 [13] Berg, P. & Haerter, J. O. Unexpected increase in precipitation intensity  
384 with temperature – a result of mixing of precipitation types? *Atmos.*  
385 *Res.* **119**, 56–61 (2011).
- 386 [14] Lenderink, G. & van Meijgaard, E. Linking increases in hourly pre-  
387 cipitation extremes to atmospheric temperature and moisture changes.  
388 *Environ. Res. Lett.* **5**, 025208 (2010).
- 389 [15] Allen, M. R. & Ingram, W. J. Constraints on future changes in climate  
390 and the hydrologic cycle. *Nature* **419**, 224–232 (2002).
- 391 [16] Pall, P., Allen, M. R. & Stone, D. A. Testing the Clausius-Clapeyron  
392 constraint on changes in extreme precipitation under CO<sub>2</sub> warming.  
393 *Clim. Dyn.* **28**, 351–363 (2007).
- 394 [17] Hardwick Jones, R., Westra, S. & Sharma, A. Observed relationships  
395 between extreme sub-daily precipitation, surface temperature, and rel-  
396 ative humidity. *Geophys. Res. Lett.* **37**, L22805 (2010).
- 397 [18] Radermacher, C. & Tomassini, L. Thermodynamic causes for future  
398 trends in heavy precipitation over Europe based on an ensemble of re-  
399 gional climate model simulations. *J. Climate* **25**, 7669–7689 (2012).
- 400 [19] Chan, S. C., Kendon, E. J., Fowler, H. J., Blenkinsop, S. & Roberts, N.  
401 M. Projected increases in summer and winter UK sub-daily precipitation  
402 extremes from high resolution regional climate models. *Environ. Res.*  
403 *Lett.* **9**, 084019 (2014).
- 404 [20] Blenkinsop, S., Chan, S. C., Kendon, E. J., Roberts, N. M. & Fowler,  
405 H. J. Temperature influences on intense uk hourly precipitation and

- 406 dependency on large-scale circulation. *Environ. Res. Lett.* **10**, 054021  
407 (2015).
- 408 [21] Kendon, E. J., Roberts, N. M., Senior, C. A. & Roberts, M. J. Realism  
409 of rainfall in a very high resolution regional climate model. *J. Climate*  
410 **25**, 5791–5806 (2012).
- 411 [22] Mizielinski, M. S. *et al.* High resolution global climate modelling; the  
412 UPSCALE project, a large simulation campaign. *Geosci. Model De-*  
413 *vel.* **7**, 1629–1640 (2014). URL [www.geosci-model-dev.net/7/1629/](http://www.geosci-model-dev.net/7/1629/2014/)  
414 [2014/](http://www.geosci-model-dev.net/7/1629/2014/).
- 415 [23] Harrison, D. L., Driscoll, S. J. & Kitchen, M. Improving precipitation  
416 estimates from weather radar using quality control and correction tech-  
417 niques. *Meteorol. Appl.* **7**, 135–144 (2000).
- 418 [24] Ban, N., Schmidli, J. & Schär, C. Heavy precipitation in a changing cli-  
419 mate: Does short-term summer precipitation increase faster? *Geophys.*  
420 *Res. Lett.* **42**, 1165–1172 (2015).
- 421 [25] Simmons, A. J., Willett, K. M., Jones, P. D., Thorne, P. W. & Dee,  
422 D. P. Low-frequency variations in surface atmospheric humidity, tem-  
423 perature, and precipitation: Inferences from reanalyses and monthly  
424 gridded observational data sets. *J. Geophys. Res.* **115**, D01110 (2010).
- 425 [26] Wright, J. S., Sobel, A. & Galewsky, J. Diagnosis of zonal mean relative  
426 humidity changes in a warmer climate. *J. Climate* **23**, 4556–4569 (2010).
- 427 [27] Pfahl, S. & Wernli, H. Quantifying the relevance of cyclones for precip-  
428 itation extremes. *J. Climate* **25**, 6770–6780 (2012).
- 429 [28] van Vuuren, D. P. *et al.* The representative concentration pathways: an  
430 overview. *Clim. Change* **109**, 5–31 (2011).
- 431 [29] Perry, M., Hollis, D. & Elms, M. *The Generation of Daily Gridded*  
432 *Datasets of Temperature and Rainfall for the UK*. Met Office National  
433 Climate Information Centre, FitzRoy Road, Exeter, Devon EX1 3PB,  
434 United Kingdom (2009).
- 435 [30] Chan, S. C. *et al.* The value of high-resolution Met Office regional  
436 climate models in the simulation of multi-hourly precipitation extremes.  
437 *J. Climate* **27**, 6155–6174 (2014).

- 438 [31] Overeem, A., Buishand, T. A. & Holleman, I. Extreme rainfall analysis  
439 and estimation of depth-duration-frequency curves using weather radar.  
440 *Water Resour. Res.* **45**, W10424 (2009).
- 441 [32] Cleveland, W. S. Robust locally weighted regression and smoothing  
442 scatterplots. *J. Amer. Stat. Assoc.* **74**, 829–836 (1979).
- 443 [33] Mishra, V., Wallace, J. M. & Lettenmaier, D. P. Relationship between  
444 hourly extreme precipitation and local air temperature in the United  
445 States. *Geophys. Res. Lett.* **39**, L16403 (2012).
- 446 [34] Efron, B. & Tibshirani, R. J. *An Introduction to the Bootstrap*, vol. 57 of  
447 *Monographs on Statistics and Applied Probability* (Chapman and Hall,  
448 New York, 1993).
- 449 [35] Exelis Visual Information Solutions. IDL (2009).
- 450 [36] R Core Team. *R: A Language and Environment for Statistical Comput-*  
451 *ing*. R Foundation for Statistical Computing, Vienna, Austria (2013).  
452 URL <http://www.R-project.org/>.

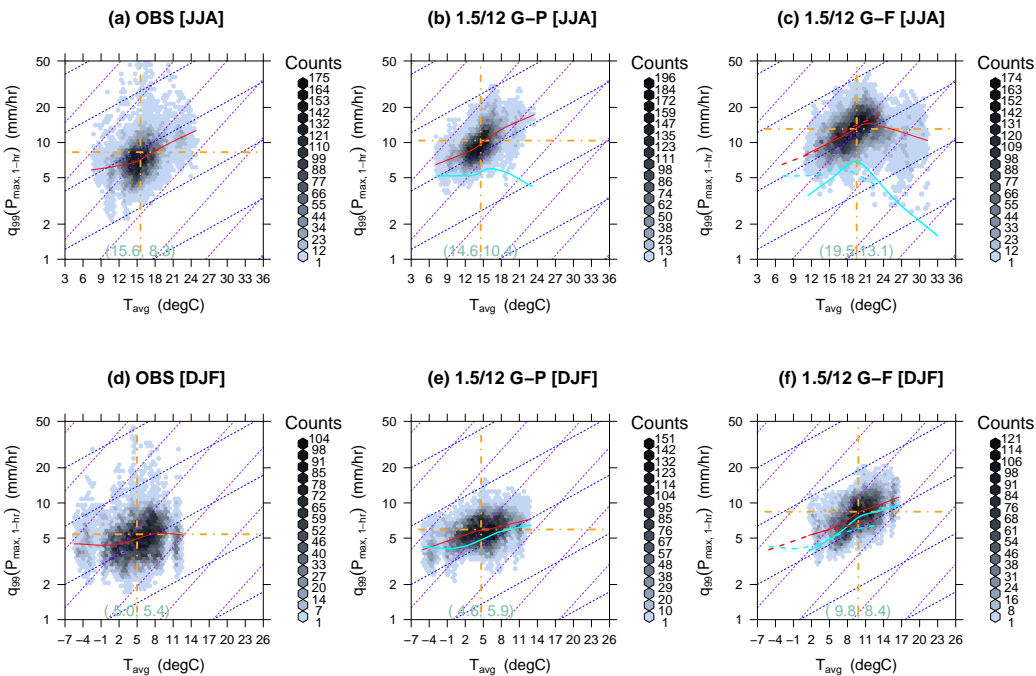


Figure 1: The relationship between surface air temperature and extreme 1-hr precipitation intensities over land. The observed (left), model-simulated present- (centre) and future-climate (right) JJA (top) and DJF (bottom) relationships between mean surface air temperature ( $T_{\text{avg}}$ ) and the 99<sup>th</sup> percentile of daily maximum 1-hr precipitation ( $P_{\text{max}, 1\text{-hr}}$ ). Red lines indicate the relationship between the two variables for the observations and 1.5-km RCM, and the orange lines indicate the mean. The 12-km RCM relationships are indicated by cyan lines. Only “wet” values (daily maximum 1-hr intensity exceeding 0.1mm/hr; see Methods) are examined. The relationship for the present-climate simulation is shown in the right (future-climate) panel as a dotted line. Blue and purple dashes indicate 1 $\times$  and 2 $\times$  C-C scaling respectively.



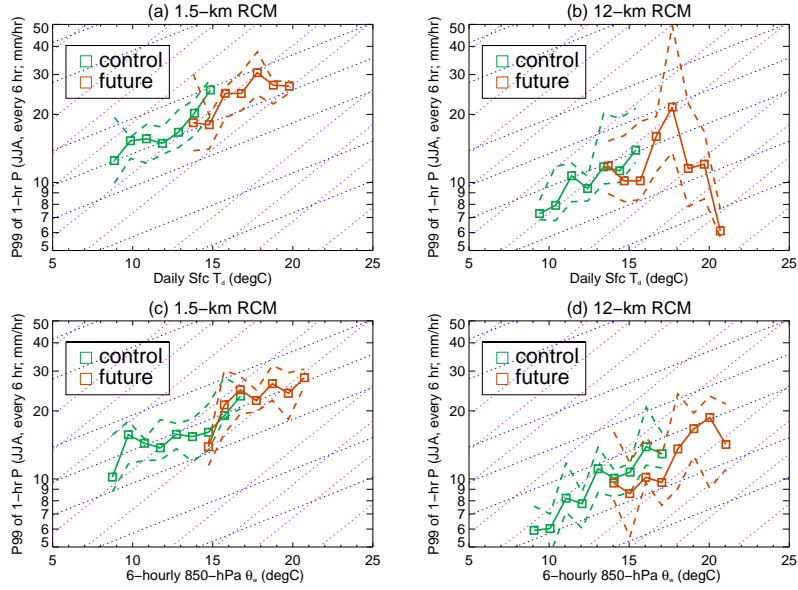


Figure 2: The summer near-surface dew point / wet-bulb potential temperature relationships with extreme 1-hr precipitation intensities. Near-surface dew point temperature  $T_d$  (upper panels) is the daily-averaged value, and wet-bulb potential temperature  $\theta_w$  (lower panels) is the instantaneous value at 850 hPa measured every 6 hours. For both  $T_d$  and  $\theta_w$ , the highest value within a  $7 \times 7$  box centred around the precipitating grid point is selected. Coloured dashes indicate the 95% confidence interval of the relationship. The left and right panels are for 1.5- and 12-km RCM respectively. The black and purple dashes indicate  $1 \times$  and  $2 \times$  C-C scaling.

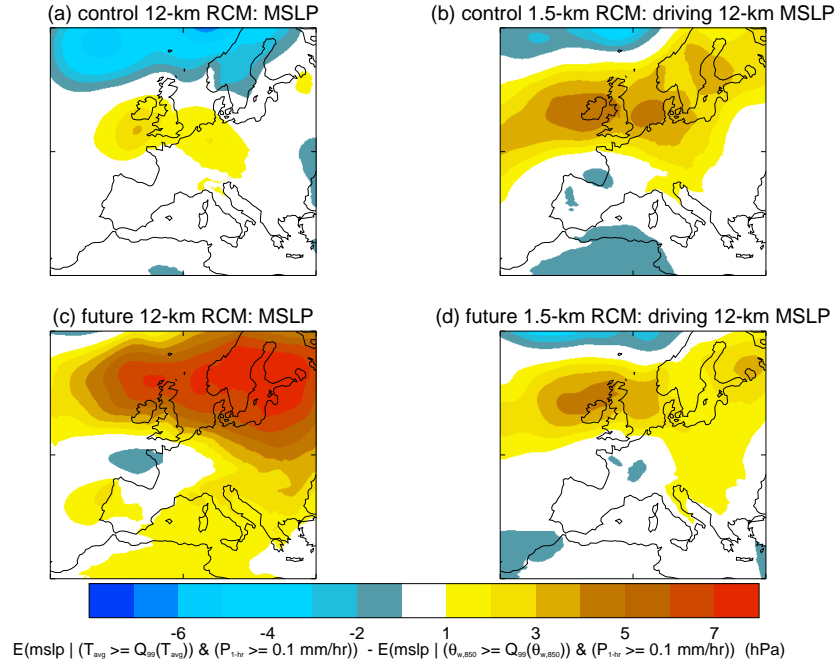


Figure 3: The mean sea-level pressure differences between wet hot days and wet hot humid days with high 850-hPa  $\theta_w$  over the southern UK. These are defined as days from any month with precipitation  $\geq 0.1\text{mm/dy}$ , and  $T_{\text{avg}}$  or 850-hPa  $\theta_w$  exceeding the 99<sup>th</sup> percentile, respectively. Only days with at least one southern UK land grid point exceeding 0.1mm/dy precipitation are selected. For 850-hPa  $\theta_w$ , we use the values from the non-local scaling analysis. However, for  $T_{\text{avg}}$ , we use the values at the precipitating grid box. For the 1.5-km RCM case, we use the MSLP that is prescribed by the driving 12-km RCM. Units are in hecto-pascals (hPa).